



Incorporation of nickel particles into a polyaniline thin film for non-enzymatic glucose sensing in alkaline medium

Ouafia Belgherbi^{1,2} · Meriem Messaoudi¹ · Hamza Bezi² · Lamria Seid² · Dalila Chouder² · Leila Lamiri^{1,3} · Assia Tounsi^{1,3} · M. Saeed Akhtar⁴ · M. A. Saeed⁴

Received: 25 June 2023 / Accepted: 20 August 2023 / Published online: 28 September 2023
© The Author(s), under exclusive licence to Springer Nature B.V. 2023, corrected publication 2024

Abstract

A non-enzymatic glucose sensor using a nickel particles/polyaniline composite has been synthesized on an indium tin oxide electrode. The PANi thin films were deposited onto the ITO surfaces using a repeated potential cycling technique in an aqueous solution containing aniline, sulfuric acid, and lithium perchlorate. Nickel particles were incorporated into the PANi/ITO surfaces using chronopotentiometry. Scanning electron micrograph and X-ray diffraction were employed to investigate the surface morphology and structure of the Ni-PAni composite, while Ultraviolet–visible spectroscopy was used to study the optical properties. The modified electrode was electrochemically characterized using cyclic voltammetry and impedance spectroscopy. The effect of PANi thin film thickness on the nickel deposition process has also been studied. Nickel was chosen due to its reduction potential being within the range where the PANi layer is in a reduced, non-conducting state. The electroactivity of the Ni-PAni/ITO electrode was evaluated through cyclic voltammetry and chronoamperometry and explored its potential for electrocatalytic glucose oxidation in an alkaline (NaOH) electrolyte. Excellent linearity in the peak oxidation current of glucose within the concentration range from 0.02 mM to 9 mM was observed with a high linear regression coefficient of 0.997. The Ni-PAni/ITO electrode displayed a high sensitivity of 215.8 mA mM⁻¹ cm⁻² in addition to the fast response time, which is less than 2 s. These results suggest that the Ni-PAni composite has the potential to be an effective electrode material to develop a cost-effective glucose sensor.

✉ Ouafia Belgherbi
o.belgherbi@crti.dz; belgherbiwafia@gmail.com

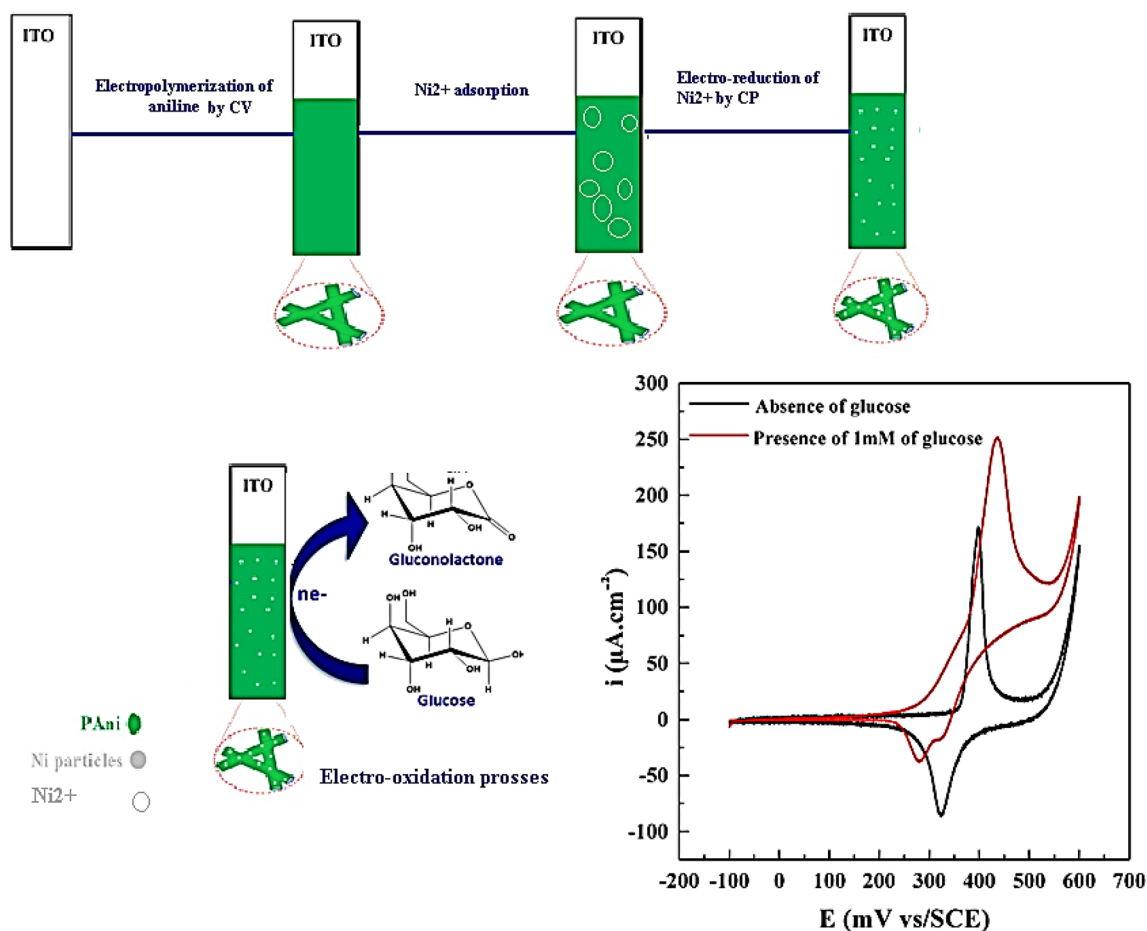
¹ Research Centre in Industrial Technologies CRTI Cheraga,
P.O. Box 64, 16104 Cheraga, Algeria

² Laboratoire d’Énergétique et d’Electrochimie du Solide
(LEES), Département de Génie des Procédés, Faculté de
Technologie, Université Sétif-1, Sétif, Algeria

³ Present Address: Laboratoire d’Electrochimie et Matériaux,
Département de Génie des Procédés, Faculté de Technologie,
Université Ferhat Abbas Sétif, 19000 Sétif, Algeria

⁴ Physics Department, Division of Science & technology,
University of Education, Lahore, Pakistan

Graphical abstract



Schematic illustration of the preparation of Ni-polyaniline electrode for glucose sensing

Research Highlights

- Nickel nanoparticles were incorporated in the polyaniline thin films by chronopotentiometry method.
- The prepared Ni-polyaniline hybrids materials exhibit high sensitivity of $215.8 \text{ mA mM}^{-1} \text{ cm}^{-2}$

- low-response time (2 s), good linearity in the concentration range from 0.1 mM to 12 mM, and low detection limit (0.01mM, S/N = 3).
- The good analytical performance, low cost, and facile fabrication method make this new electrode material promising for the development of effective glucose sensors.

Keywords Composites materials · Electrodeposition · Glucose oxidation · Modified electrode · Nickel particles · Polyaniline thin films

1 Introduction

In, the past few decades, the creation of sensors exhibiting high sensitivity, selectivity, speed, and reliability to detect chemical or biological species has been an area of intense research interest. Glucose, a vital component of carbohydrates and a key source of energy for human metabolism is

a particularly important analyte. Detecting glucose is vital not just for diabetes diagnosis, but also in industries such as food and pharmaceuticals [1–5]. Electrochemical, chromatographic, and fluorescent techniques have been employed for both intermittent and continuous glucose detection [6]. Among these, electrochemical sensor is a type of sensor that outputs the changes produced by the target substance in the

form of an electrical signal. Compared with other detection methods, electrochemical analysis does not require large analytical instruments, has fast reaction speed, high sensitivity and selectivity, and can be used for real-time monitoring of target analytes. Because of these advantages, electrochemical analysis is widely used in environmental detection, food industry, and biomedical fields [7]. In practical electrical analysis and detection, the standard three-electrode system is usually used [8]. Electrochemical glucose sensors can be divided into three types: potentiometric, amperometric, or conductometric sensors.

The electrochemical detection can be categorized as enzymatic or non-enzymatic. Previous studies have predominantly utilized GOx and other enzymes for glucose biosensors [9, 10]. However, the instability of enzymatic glucose sensors due to the intrinsic properties of enzymes poses a serious challenge. Enzyme activity can be significantly impacted by factors such as temperature, pH, oxygen, humidity, and exposure to toxic chemicals, thereby limiting their applicability [11]. In contrast, non-enzymatic glucose sensors have gained research interest due to their advantages of low cost, high stability, fast response, and low detection limit [12, 13]. Metals like Pt [14], Ag [15], Au [16], and 3D transition metals like Co [17], Fe [18], and Cu [19], are commonly utilized as electrodes to improve electrocatalytic activity. Nevertheless, the high cost of noble metals and the restricted usefulness caused by surface contamination by intermediates pose significant drawbacks. Polyaniline (PAni) was utilized as a cost-effective matrix to disperse metal particles in glucose sensing electrodes, due to its low density and higher surface area reaction [20, 21]. Composite materials composed of π -conjugated polymers (CPs) and metal particles (MPs) are of great interest to researchers [22, 23]. The properties of these materials are unique and can be combined to enhance physical and chemical properties that would enable them to be a potential candidate for many applications in the areas of nanoscience and nanotechnology. Recent studies have focused on developing new composites of conducting polymers and metal particles to generate materials with novel properties and potential applications. The goal of this study is to create a novel electrochemical non-enzymatic sensor that is based on a conjugated π polymer (polyaniline) and functionalized with the addition of nickel particles. The proposed sensor exhibits strong catalytic performance in the context of the oxidation of glucose.

2 Experimental methods

2.1 Chemicals

Chemicals like; aniline ($C_6H_5NH_2$), sulfuric acid (H_2SO_4), nickel sulfate ($NiSO_4$), sodium sulfate (Na_2SO_4), glucose

($C_6H_{12}O_6$, H_2O), and sodium hydroxide (NaOH), were purchased from Sigma-Aldrich and were used without further purification. Lithium perchlorate ($LiClO_4$) was purchased from Fluka. Distilled water was used to prepare all aqueous solutions.

2.2 Synthesis methodology

Potentiostat/Galvanostat Voltalab PGZ 301 was used at room temperature for electrochemical tests performed in a standard 3-electrode system without agitation. A saturated calomel electrode was used as a reference electrode while platinum wire serves as a counter electrode. The ITO, PAni/ITO, and Ni-PAni/ITO were used as working electrodes. The ITO substrates ($1 \times 1 \text{ cm}^2$) pre-cleaned through sonication in acetone, ethanol, and water for 15 min each was used to prepare modified electrodes. Afterward, the purified working electrode was submerged in a solution containing aniline (0.1M) dissolved in sulfuric acid (0.5M), with a supporting salt of lithium perchlorate ($LiClO_4$). The PAni coatings were washed with distilled water and dried in an ambient atmosphere. To create Ni-PAni/ITO thin films, the electrodeposition of nickel onto the PAni/ITO samples was conducted by a galvanostatic process using a solution containing $NiSO_4$ (0.1M) and Na_2SO_4 (0.1M). The SEM micrographs were used to study the microstructure and surface morphology of the Ni-PAni composites. The electrochemical properties of the samples were investigated through Cyclic Voltammetry and electrocatalytic activity for glucose oxidation was investigated in NaOH (0.1M) electrolytic solution. The thickness of the films was measured by a mechanical profilometer of the KLA Tecnor Alpha-Step D-500 type.

3 Results and discussion

3.1 Electro-polymerization of aniline

The cyclic voltammetry method was used to investigate the electrodeposition of PAni thin films onto the ITO substrate. These PAni thin films with a thickness of 100 nm were used as a matrix to prepare composite thin films. The cyclic voltammetry was performed at a scan rate of 10 mV/s with a potential ranging from -0.2 and 0.9 V. Figure 1a and b illustrate the outcomes of the very first cycle and the five succeeding cycles, respectively. During the positive scan, a current density increase was detected at 0.85 V, which is believed to be caused by monomer oxidation [24]. The following reverse scan indicated a current loop, indicating the nucleation and growth of the PAni film. The crossover between the cathodic and anodic branches indicated the

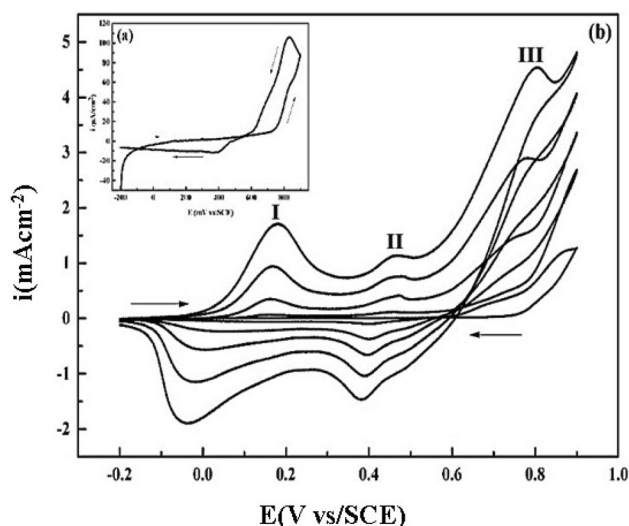


Fig. 1 Cyclic voltammogram of electropolymerization of aniline on ITO electrode **(a)** first cycle and **(b)** 5 continuous cycles. Scan rate 10 mV/s

presence of a new phase. With an increase in the number of cycles, the deposition rate of polyaniline onto the working electrode was observed to increase, as evident from the new oxidation and reduction peaks appearing in Fig. 1b. The peak appearing at less positive potentials (I) is attributed to the oxidation of leucoemeraldine (a fully reduced form of PANi) to emeraldine (a half-reduced form of PANi). On the other hand, the intermediate peak (peak II) appearing around 0.45V is usually assigned to degradation products (p-benzoquinone) and later to its oxidation. The peak (III) is related to the oxidation of emeraldine to pernigraniline (a fully oxidized form of PANi) [25]. Following the electro-polymerization process, the ITO substrate was entirely coated with a transparent green film.

3.2 Incorporation and characterization of nickel particles on polyaniline thin films

3.2.1 Electrodeposition of Ni particles on PANi electrode

The chrono-potentiometric curve for galvanostatic electrodeposition of nickel within the polyaniline matrix is shown in Fig. 2. The electrodeposition time was fixed at 60 s while the intensity of the applied current was set at -0.1 mA. The chrono-potentiometric curve obtained from the electrodeposition of nickel in the polyaniline matrix by the galvanostatic method can be divided into three steps. In step I, the potential of the electrode increases rapidly due to the charge of the double layer. Step II is characterized by the maximum potential value, which corresponds to the reduction potential of the metal ions (Ni^{2+}) and marks the beginning of the

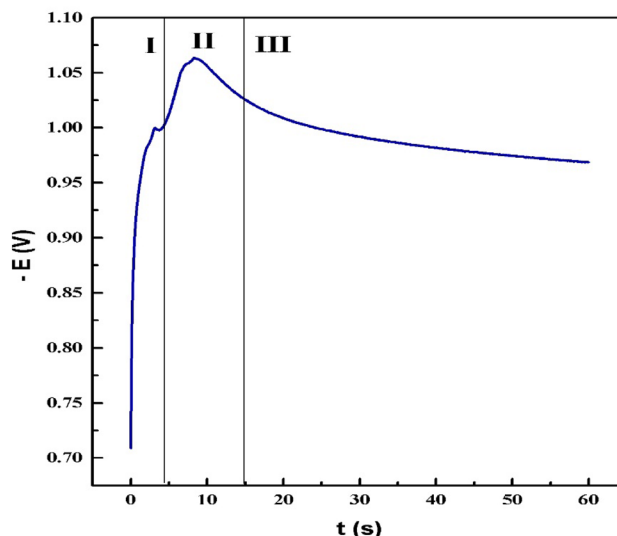


Fig. 2 Electrodeposition of nickel on polyaniline by the galvanostatic method. Applied current intensity = -0.1 mA, $t=60$ s

nucleation of nickel on the working electrode. Finally, in step III, the potential decreases and reaches a stable plateau due to a pseudo-stationary regime, where the electrodeposition of nickel continues on the polymer surface.

3.2.2 Impedance spectroscopy

The impedance measurements were carried out on polyaniline films synthesized by the potentiostatic method in the frequency range from 100 kHz to 100 MHz before and after the incorporation of nickel particles in $\text{LiClO}_4/\text{H}_2\text{SO}_4$ solution. Figure 3a and b display the Nyquist plots

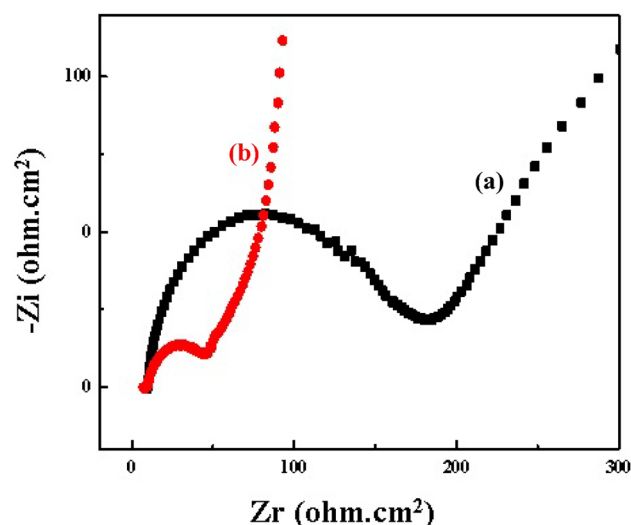


Fig. 3 Nyquist diagrams obtained in a solution (0.1 M of $\text{LiClO}_4/0.5$ M of H_2SO_4): **a** PANi/ITO, **b** Ni-PANi/ITO

Table 1 Results of the measurement of the conductivity of PANi and Ni-PANi

Material	σ (S/cm)
PANi	456×10^{-4}
Ni-PANi	390×10^{-3}

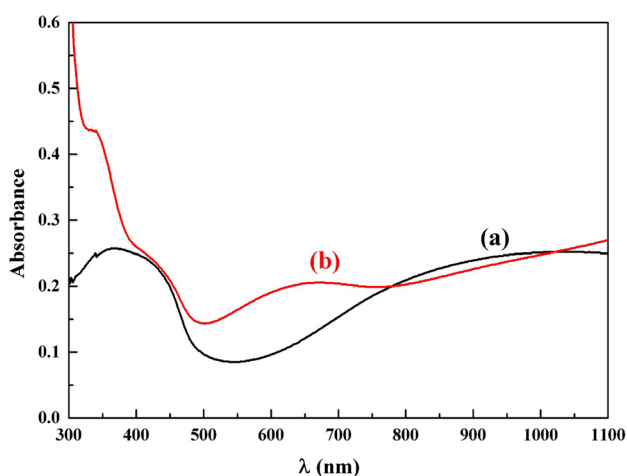
for polyaniline thin films. The high-frequency semicircles indicated the charge-transfer-driven process followed by a low-frequency straight line specific to a diffusion process. The charge transfer resistance decreases from 172.2 to 134.4 $\Omega \text{ cm}^2$ after the incorporation of nickel particles into the polymer. These results are consistent with previous studies and indicated the incorporation of nickel particles into the polymer that ultimately enhances the electrochemical behavior of composites.

3.2.3 Electrical characterization by the four-point method

The electrical properties of the polyaniline and Ni-PANi composite films, such as electrical resistivity and conductivity, were analyzed using a four-point measuring device at room temperature. The measurement involved supplying a constant current source to the sample and measuring the resulting potential difference. The conductivity of the Ni-PANi composite was found to be significantly higher than that of polyaniline alone. These results were consistent with impedance spectroscopy studies, which showed a decrease in the diameter of the circular arc. Therefore, it can be concluded that nickel improves the conductivity of the polymer, as summarized in Table 1.

3.3 UV–visible spectroscopy

UV–Vis spectroscopy was used to study the interaction between the PANi and Ni nanoparticles deposited on the ITO substrate (Fig. 4a). As can be seen in Fig. 4a, three

**Fig. 4** UV–visible spectra of the films of **a** PANi and **b** Ni-PANi/ITO

particular peaks of polyaniline at 362, 434, 953 nm are attributed to $\pi\pi^*$, polaron- π^* , and π - polaron transitions, respectively. This illustrates that the electrodeposited PANi films were in emeraldine salt form [26]. Therefore, in comparison to the peaks of the PANi films, we observed a significant change in all absorption peaks, which are shown in Fig. 4b for Ni-PANi, and are as follows: 338, 434, 654, the peak shifts observed confirmed the interaction of Ni with the amine sites of the polyaniline, which is consistent with the results reported by Mrinmoy Goswami et al. [27].

3.4 Microstructure morphology and structural analysis

An SEM image was obtained for the samples before and after nickel deposition for 60 s, as shown in Fig. 5. The image reveals two distinct morphologies: the fibrous morphology of the polyaniline and the spherical morphology of the nickel particles, which are dispersed on the surface of the polyaniline. This observation is consistent with results reported by O. Belgherbi et al. [28]. The actual size, which consist of diameter and area of Ni particles were calculated using imageJ software. In addition, the percentage of all appeared particles on the surface of polyaniline thin films was estimated. The obtained results are listed in Table 2. It is found that the average diameter and average surface of Ni particles are 0.91 μm and 0.77 μm^2 , respectively.

To verify the existence and quality of the nickel deposition, X-ray diffraction (XRD) analysis was performed on a nickel-modified polyaniline thin film. The XRD pattern revealing well-defined diffraction peaks is presented in Fig. 6. The diffraction peaks appeared at 2θ of 45.66° and 50.92° corresponding to the (111) and (200) planes, respectively of the face-centered cubic phase of nickel in accordance with the JCPDS # 00-004-0850. Furthermore, the diffraction peaks at 2θ values of 30.34°, 35.33°, and 60.47° correspond to the crystal structure of the ITO substrate (JCPDS file no. 98-005-0849). Additionally, there is a peak located at (2θ): 21.48°, which corresponds to the crystal structure of polyaniline.

The average size of the crystallites has been estimated to be 35.07 nm using Scherrer's formula (Eq. 1) for the cubic plane with centered faces (200).

$$D = \frac{0.9\lambda}{B\cos\theta} \quad (1)$$

The variables ' D ', ' B ', ' λ ', and ' θ ' represent the crystallite size, full width at half maximum, the wavelength of X-rays, and Bragg's diffraction angle, respectively.

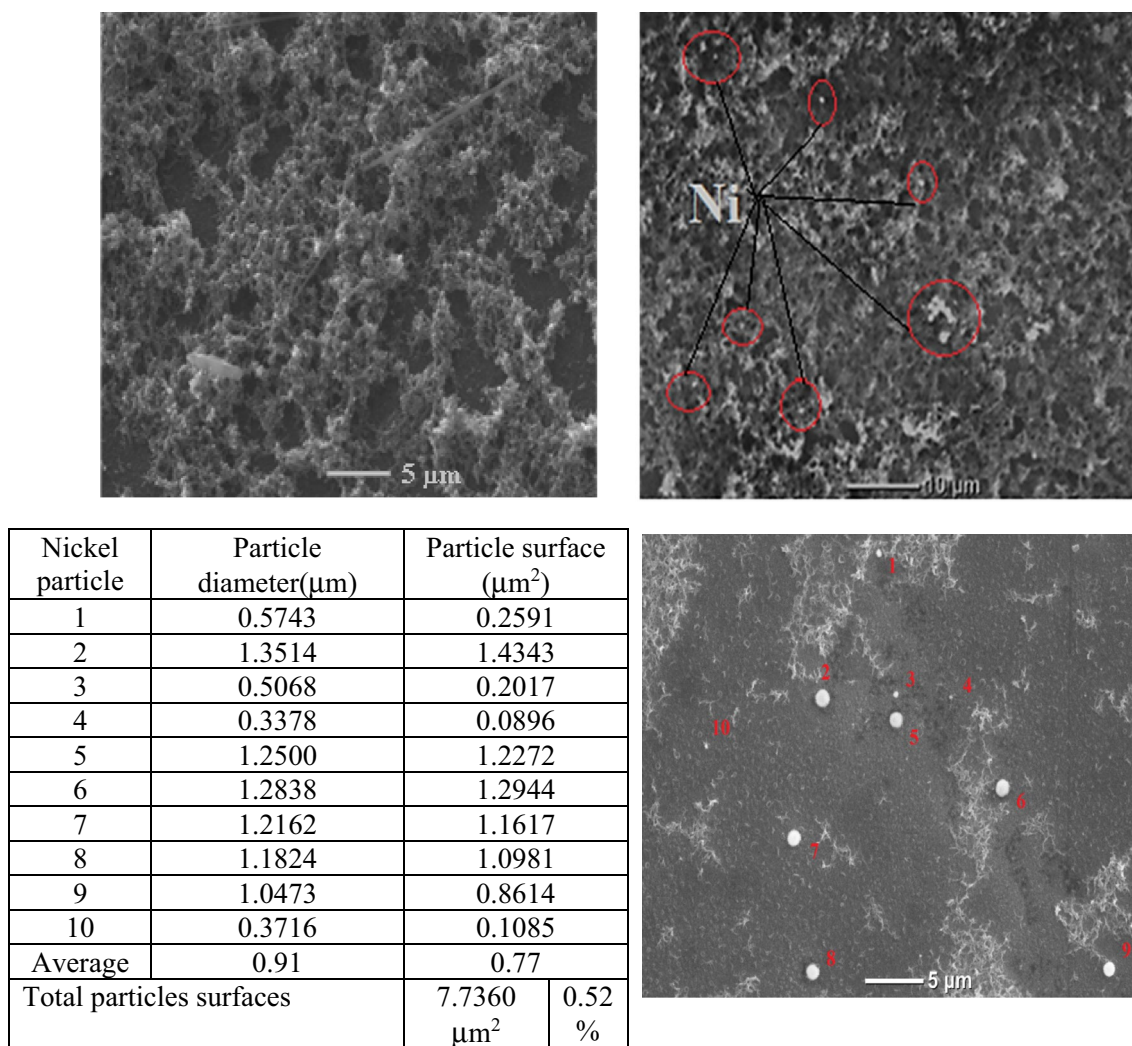


Fig. 5 SEM images obtained after nickel deposition on PANi for 60 s at -0.1mA in a 0.1 M NiSO_4 solution

Table 2 Results of the average diameter and average area of Ni particles deposited onto polyaniline thin films

Nickel particle	Particle diameter(μm)	Particle surface (μm^2)
1	0.5743	0.2591
2	1.3514	1.4343
3	0.5068	0.2017
4	0.3378	0.0896
5	1.2500	1.2272
6	1.2838	1.2944
7	1.2162	1.1617
8	1.1824	1.0981
9	1.0473	0.8614
10	0.3716	0.1085
Average	0.91	0.77
Total particles surfaces		7.7360 μm^2 0.52%

3.5 The modified electrode's electrochemical performance concerning the oxidation of glucose

3.5.1 Electrochemical glucose sensing

Numerous methods have been devised for detecting glucose, such as conductometry, colorimetry, electrochemistry, fluorescent spectroscopy, and optical rotation [29]. Electrochemical techniques are particularly popular due to their simplicity, selectivity, and portability. According to previous studies, biosensors based on electrochemical techniques offer several benefits, including low detection limits, rapid response times, high stability, and affordability [30]. Currently, electrochemical sensing is commonly used to monitor glucose levels, particularly in amperometric mode, due to its affordability, high stability,

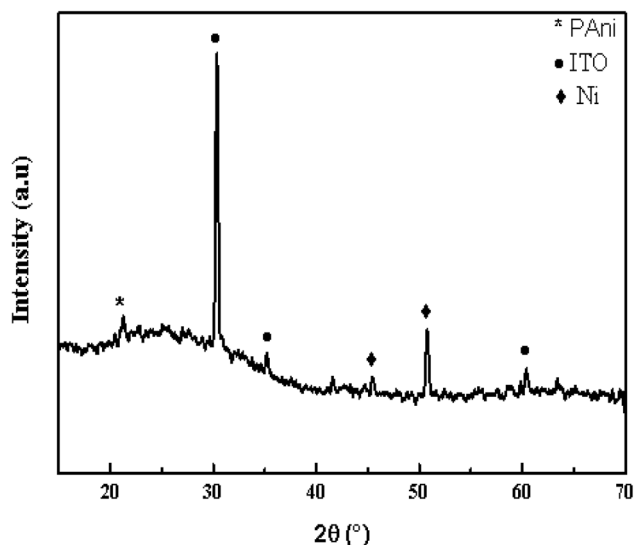


Fig. 6 X-ray diffraction diagrams of Ni-PANI composite film deposited on ITO substrate

rapid response time, and low detection limit. To measure glucose levels, a tiny blood droplet is positioned onto a disposable electrochemical test strip containing the reference, working, and auxiliary counter electrodes. The working electrode is given a fixed potential, and enzymes that have been immobilized on the electrode respond with glucose in the blood to create a current flow and electrons. The resulting electric charge or current moving through the electrode is relative to the glucose concentration and can be measured accurately.

3.6 Electrochemical activity of Ni-PANI/ITO

3.6.1 Cyclic voltammetry behavior

Cyclic voltammetry was utilized to study the polarization characteristics of PANi thin films modified with nickel in a NaOH (0.1 M) solution, with a scan rate of 15 mVs^{-1} (Fig. 7). The initial positive scan revealed a comparable trend to pure Ni [31]. We noticed that the peak currents for oxidation displayed an increase with the rise in cycle numbers, excluding the first cycle, implying an increase in activation sites. Moreover, the oxidation peak potentials shifted toward a negative direction, potential displacement of the anode and cathode peaks toward lower values which approves the electro-catalytic effect of the OH^- species on the electrochemical behavior of the electrode. As has already been indicated in the literature [32], species such as (NiOOH) are the entities involved in the electro-catalytic process and that the oxygen discharge rate is significantly influenced by the alkalinity of the medium.

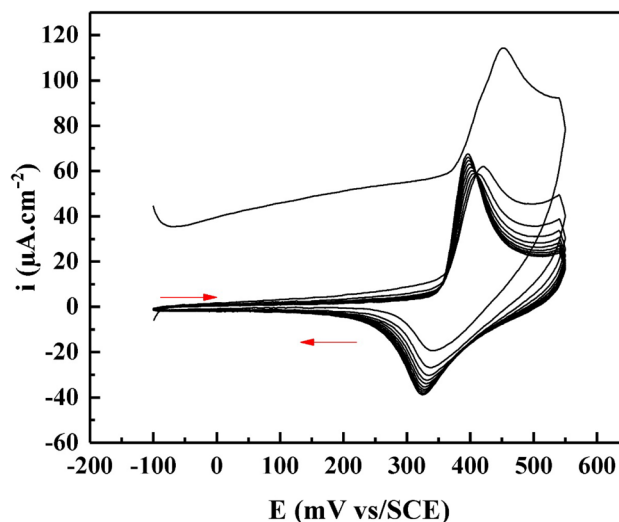


Fig. 7 Cyclic voltammograms of Ni-PANI/ITO in a 0.1M NaOH solution, $V_b = 15 \text{ mVs}^{-1}$ during 10 cycles

The expansion of nickel electrodes is a known consequence of the formation of the NiOOH phase. This phase has a lower interelectrode spacing, resulting in reduced internal resistance. Consequently, it is commonly regarded as a superior electroactive material that offers high electrochemical performance.

Figure 8a shows a series of cyclic voltammetry scans performed on an electrode modified with Ni-PANI in NaOH (0.1 M) as a supporting electrolyte at scanning speed in the range from 5 to 700 mV s^{-1} . The current density was observed to increase with increasing scanning speed. Figure 8b illustrates the relationship between the oxidation peak and the square root of the scanning speed. The intensity of the oxidation and reduction peaks showed a linear correlation with the square root of the scanning speed, indicating that the reactions occurring on the modified electrode were reversible. This indicates that mass transfer in the double-layer region of the electrodes is primarily a diffusion-controlled electrochemical process, which is ideal for glucose detection. These observations are consistent with the previous studies [33].

3.7 Electrocatalytic oxidation of glucose at the Ni-PANI/ITO electrode

The electrocatalytic performance of the Ni-PANI/ITO electrode was assessed by obtaining cyclic voltammograms in the presence and absence of glucose (Fig. 9). In the absence of glucose (curve a), the Ni-PANI/ITO electrode exhibited a couple of well-defined redox peaks. However, upon the addition of glucose (1 mM) to the NaOH (0.1 M) solution, a significant increase in the anodic peak current was observed (curve b). On the other hand, the cathodic peak current

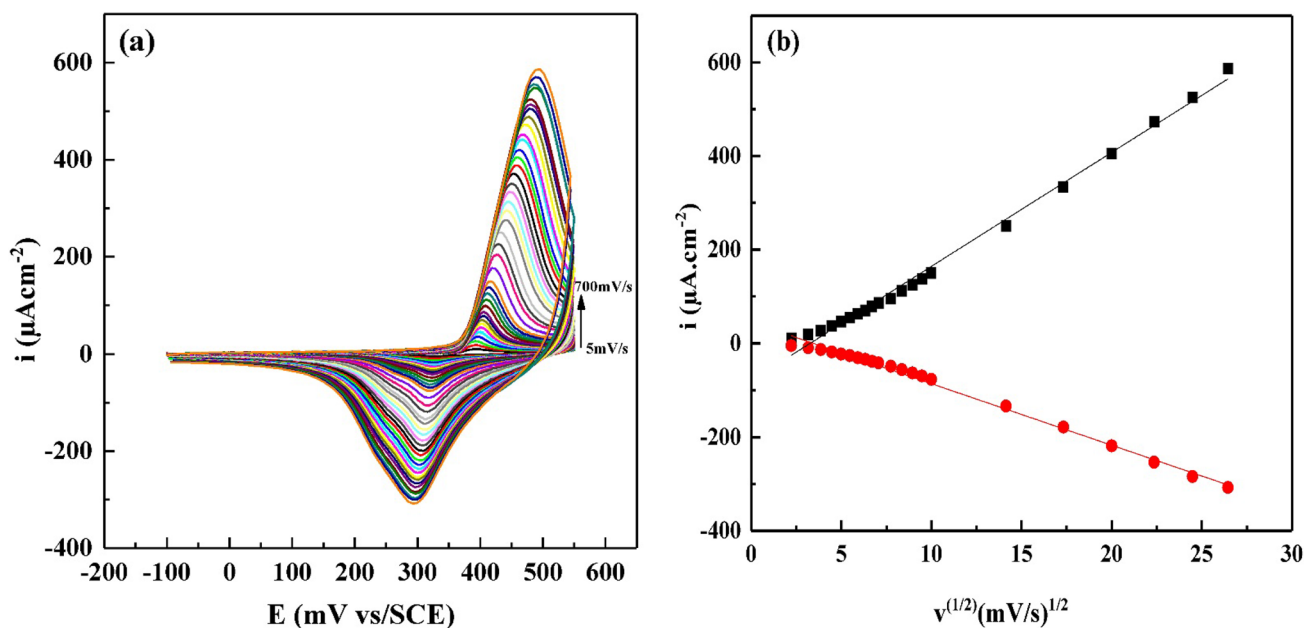


Fig. 8 Cyclic voltammetry curves plotted on the Ni-PAni/ITO electrode at different scan rate in a 0.1M NaOH solution (a), Variation in the intensity of the oxidation peak and reduction as a function of the square root v (b)

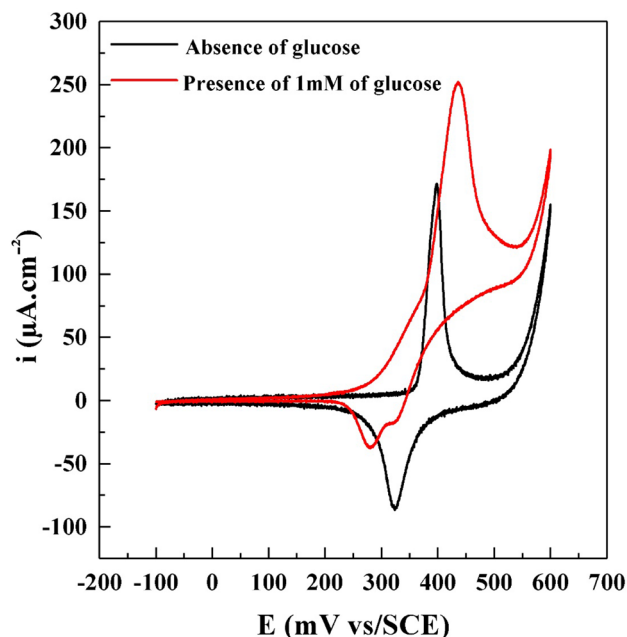
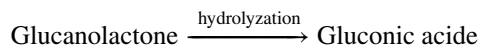
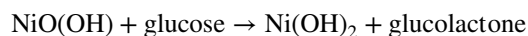
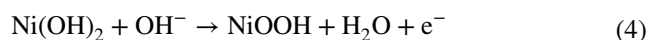
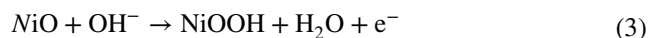
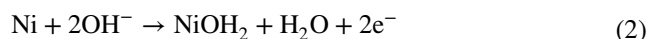
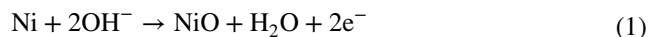


Fig. 9 Cyclic voltammetry curve recorded on the Ni-PAni/ITO electrode in a 0.1 M NaOH solution in the absence (a) and in the presence (b) of glucose

decreased, which suggests that Ni-PAni/ITO can catalyze glucose oxidation, the potential displacement in the presence of glucose indicating that the material was sensitive to the analyte added to the system by the generation of the more active sites competing for the OH^- available with the

composite surface, which could be essential to improve the catalyst. These findings demonstrate the electrocatalytic potential of the Ni-PAni/ITO electrode for glucose detection. Previous research has also suggested that the oxidation of glucose to gluconolactone is catalyzed by the Ni(III)/(II) redox couple, as described in the literature [34].



The oxidation of glucose on the Ni-PAni/ITO electrode occurs via rapid reduction of Ni(III) to Ni(II) species.

3.8 Effect of thickness of polyaniline

The impact of polyaniline thickness on the electrocatalytic effectiveness of the Ni-PAni/ITO modified electrode toward glucose oxidation was examined and shown in Fig. 10. The cyclic voltammograms observed between -0.1 and 0.7 V

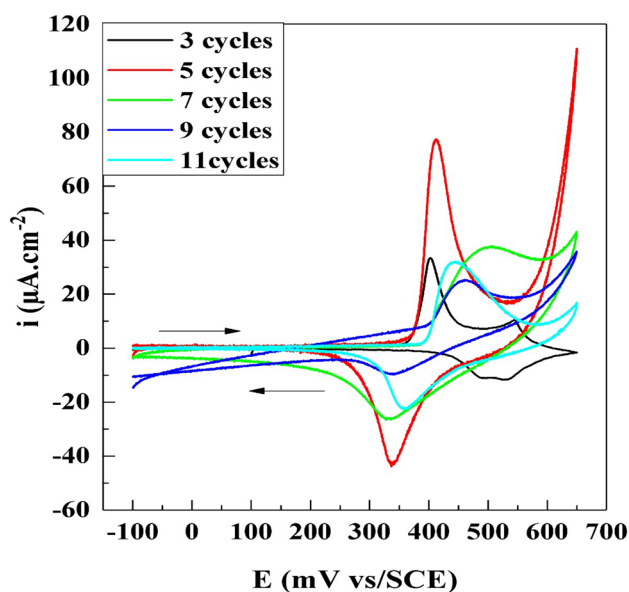


Fig. 10 Cyclic voltammograms recorded on three Ni-PAni/ITO electrodes prepared at different polyaniline cycle numbers: 3, 5, 7, 9, and 11 cycles. Medium: 0.1M NaOH, containing 1mm glucose

illustrated a redox pair related to the oxidation of Ni(II) to Ni(III) and reduction of Ni(III) to Ni(II). The oxidation current density was observed to decrease as a function of polyaniline film thickness. This decrement would result from the reduction in the effective area of modified electrodes. Therefore, for subsequent experiments, Ni-PAni/ITO-modified electrodes with an electrodeposition thickness of 100 nm were used.

3.9 The influence of the deposition time

Optimization of the Ni electrodeposition time is crucial for glucose sensing using Ni-PAni/ITO-modified electrodes. Figure 11 depicts the response of modified electrodes toward the addition of glucose (1 mM) with varying Ni electrodeposition time from 60 to 180 s in NaOH (0.1 M) solution. It is evident that the electrodeposition time of 60 s. yielded the highest response, as indicated by the highest oxidation current density. Longer deposition times such as 90, 120, and 180 s resulted in gradually decreased current densities, possibly due to the generation of larger Ni and even aggregation, which could offset the advantage of a larger surface area. This observation is consistent with previous findings by other authors [35].

3.10 Electrochemical behavior of the Ni-PAni/ITO electrode and glucose detection calibration curve

The detection of glucose by Ni-PAni/ITO electrodes was assessed by obtaining cyclic voltammograms in NaOH

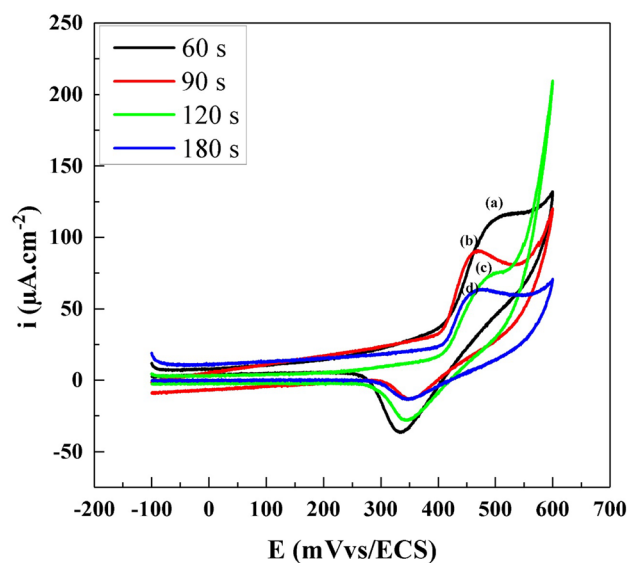


Fig. 11 Cyclic voltammograms recorded on four Ni-PAni/ITO electrodes prepared with different nickel-deposition times: 60, 90, 120, and 180 s in 0.1 M NaOH medium containing 1 mM of glucose

(0.1M) at different concentrations of glucose as depicted in Fig. 12a. The intensity of the oxidation peak gradually increased with increasing glucose concentration, indicating an electrocatalytic oxidation process. However, the peak intensity started to decrease at a glucose concentration of 11 mM due to electrode saturation. The obtained data were used to plot the corresponding calibration curve as presented in Fig. 12b. The response signal of the Ni-PAni/ITO electrode increased consistently with increasing glucose concentration, indicating a typical electrocatalytic oxidation process. The current density for oxidation exhibits a linear relation with high correlation coefficients ($R^2 = 0.99$) for glucose concentration in the ranges of 0.02–0.1 mM and 1–8 mM. The electrode's detection limit was determined to be 0.01 mM, and its sensitivity was approximately $171.5 \mu\text{A mM}^{-1} \text{cm}^{-2}$. The electrode's analytical performance was compared with those of recent works for glucose detection, and the results are summarized in Table 3, indicating that our electrode's performance is comparable to others.

3.11 Influence of the scanning speed on the oxidation of glucose

Figure 13a represents the cyclic voltammograms obtained at various scanning rates for the Ni-PAni/ITO electrode to access the effect of scan rate on the oxidation current. The variation in scanning rate during glucose oxidation increased the oxidation peak intensity and a shift in the oxidation potential toward positive values. Figure 13b represents a linear relationship between the intensity of the oxidation peak and the square root of the scanning rate

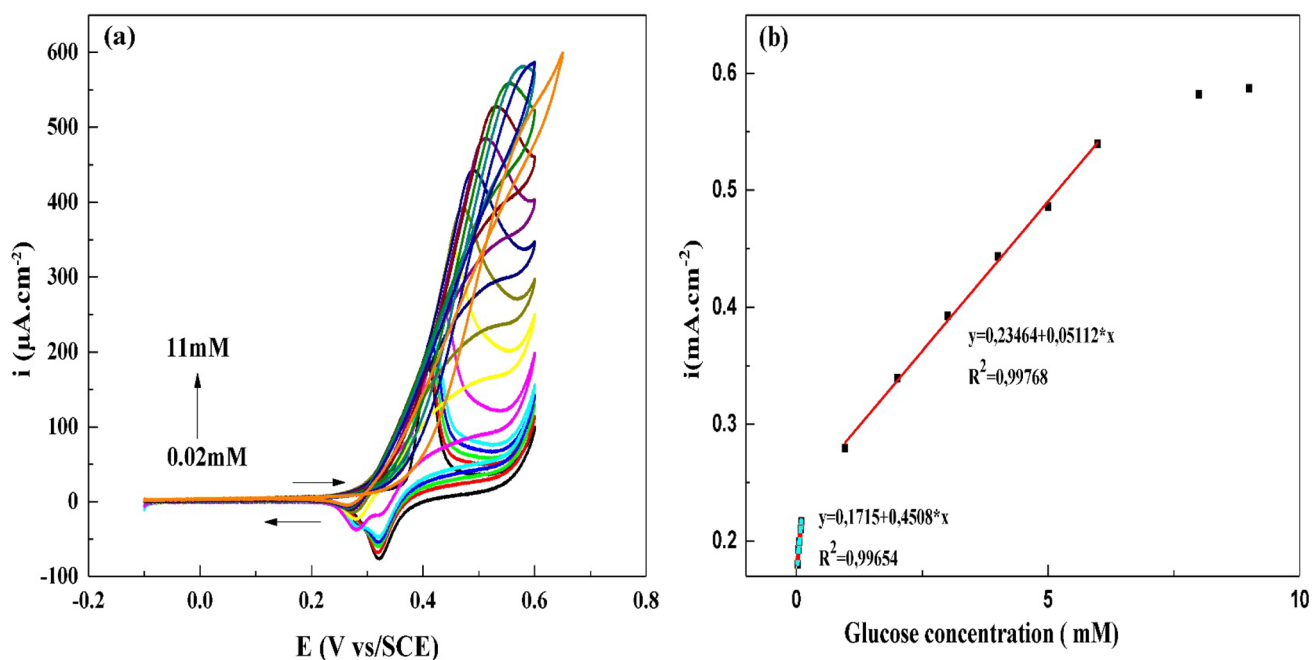


Fig. 12 **a** Variation in the response of the Ni-PAni/ITO electrode following the successive injection of different concentrations of glucose in a 0.1 M NaOH solution. **b** Calibration curve of the sensor response

Table 3 Comparison of the analytical performances of the Ni-PAni/ITO sensor with those of other materials used for the determination of glucose

Electrode material	Detection limit (μM)	Sensitivity ($\mu\text{A mM}^{-1} \text{cm}^2$)	Domain of linearity (mM)	References
RGO-Ni(OH) ₂	0.6	11.43	0.00313–3.05	[36]
NiO-Graphene	5	–	0.02–10	[37]
RGO-Ni NPs	5	–	0.0002–2.1	[38]
Ni-MWCNTs	0.89	67.2	0.003–17.5	[39]
Ni-PAni/ITO	10	171.5	0.02–0.1	In this work

suggesting that the glucose oxidation reaction on the surface of the PAni-Ni/ITO electrode is controlled by a diffusion process.

3.12 Ni-PAni/ITO electrode performance

The chronoamperometry technique was used to investigate the effect of various materials on the detection of glucose. The electrode (Ni-PAni/ITO) was exposed to a potential (0.45 V) in a NaOH solution (0.1M) that contains glucose (1mM) and other materials like hydrogen peroxide (H₂O₂), ascorbic acid (AA), sucrose (Sac), and KCl with 0.1mM concentration. The variation in current as a function of time was recorded and plotted as $i = f(t)$, Fig. 14. It can be observed that there is no significant change in the chronoamperometry curves of the Ni-PAni/ITO electrode in the presence of KCl, sucrose, ascorbic acid, and hydrogen peroxide. This suggests that the oxidation of glucose is not affected revealing that

Ni-PAni/ITO electrode exhibits excellent selectivity for the detection of glucose.

4 Conclusion

We have described a straightforward electrochemical technique for fabricating nickel-polyaniline composite thin films. This method offers a promising and uncomplicated approach to creating a uniform distribution of nickel particles within the polyaniline matrix. The synthesized composites serve as an effective catalyst for the electro-oxidation of glucose in a NaOH (0.1M) solution. Overall, the results demonstrate the potential of the Ni-PAni electrode as one of the promising candidates for non-enzymatic glucose sensing applications. Further studies could focus on the optimization of the electrode fabrication process and the investigation of its long-term stability and reproducibility. Additionally, the

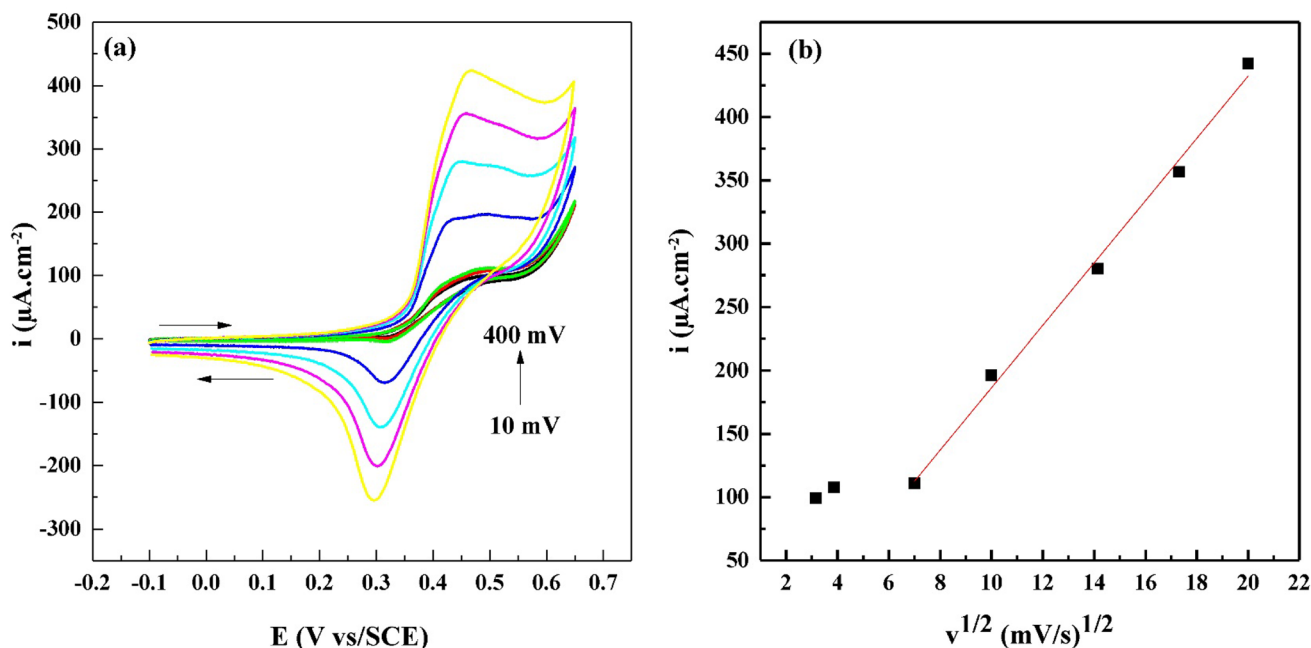


Fig. 13 **a** Cyclic voltammograms plotted on the Ni-PAni/ITO electrode at different scan rate in a 0.1 M NaOH solution containing 1 mM of glucose. **b** Variation in the intensity of the glucose oxidation peak as a function of the square root of v

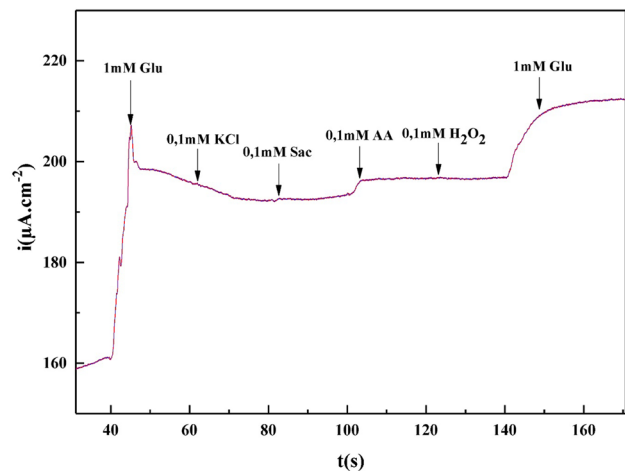


Fig. 14 Amperometric response of the Ni-PAni/ITO electrode in a 0.1 M NaOH solution with successive injections of the analytes: Glc, KCl, Sac, AA, and H_2O_2

electrode's performance could be evaluated in real samples to determine its practical utility for glucose detection.

Author contributions All authors reviewed the manuscript."

Declarations

Competing interests The authors declare no competing interests.

References

1. Qiao WM, Zhao Y, Liang H, Li J, Luo TS, Lu YS, Shi S, Lu X, Sun W, Ping X (2020) Electrochemical non-enzymatic glucose sensors: recent progress and perspectives. *Chem Commun.* <https://doi.org/10.1039/d0cc05650b>
2. Vernekar PR, Purohit B, Shetti NP, Chandra P (2021) Glucose modified carbon paste sensor in the presence of cationic surfactant for mefenamic acid detection in urine and pharmaceutical samples. *Microchemistry.* <https://doi.org/10.1016/j.microc.2020.105599>
3. Rostami-avanroudi S, Babakhanian A (2021) New electrochemical sensor for direct quantification of vitamin K in human blood serum. *Microchem J.* <https://doi.org/10.1016/j.microc.2020.105716>
4. Ghanbary E, Asiabani Z, Hosseini N, Kiaie SH, Kaki S, Ghasempour H, Babakhanian A (2020) The development of a new modified graphite pencil electrode for quantitative detection of Gibberellic acid (GA3) herbal hormone. *Microchem J.* <https://doi.org/10.1016/j.microc.2020.105005>
5. Azizi Z, Babakhanian (2018) A fabricating a new electrochemically modified pencil graphite electrode based on acetophenone (2, 4-dinitrophenyl) hydrazone for determining selenium in food and water samples. *Anal Methods.* <https://doi.org/10.1039/C8AY01959B>
6. Schierenbeck F, Franco-Cereceda A, Liska J (2017) Accuracy of 2 different continuous glucose monitoring systems in patients undergoing cardiac surgery: intravascular microdialysis versus subcutaneous tissue monitoring. *J Diabetes Sci Technol.* <https://doi.org/10.1177/1932296816651632>
7. Zhang L, Wang J, Liu F, Xiong Y, Liu Z, Jiang D, Li Y, Tu D, Wang Y, Pu X (2017) Rapid detection of bla_{NDM-1} in multidrug-resistant organisms using a novel electrochemical biosensor. *RSC Adv.* <https://doi.org/10.1039/C6RA27916C>

8. Wei M, Qiao Y, Zhao H, Liang J, Li T, Luo Y, Lu S, Shi X, Lu W, Sun X (2021) Electrochemical non-enzymatic glucose sensors: recent progress and perspectives. *Chem Commun*. <https://doi.org/10.1039/DOCC05650B>
9. Delk S, Parsanta ASMD, Pashupulla AP, Srivastava KA, Yadav SK, Saxena S (2022) Enzyme based glucose biosensor—an overview. *J Pharm Negat Results*. <https://doi.org/10.47750/pnr.2022.13.S09.1090>
10. Radhakrishnan S, Lakshmy S, Santhosh S, Kalarikkal N, Chakraborty B, Rout CS (2022) Recent developments and future perspective on electrochemical glucose sensors based on 2D materials. *Biosensors*. <https://doi.org/10.3390/bios12070467>
11. Babulal SM, Chen SM, Palani R, Venkatesh K, Haidyrah AS, Ramaraj SK, Yang CC, Karuppiiah C (2021) Graphene oxide template based synthesis of NiCO₂O₄ nanosheets for high performance non-enzymatic glucose sensor. *Colloids Surf A*. <https://doi.org/10.1016/J.COLSURFA.2021.126600>
12. Wang F, Chen X, Chen L, Yang J, Wang Q (2019) High-performance non-enzymatic glucose sensor by hierarchical flower-like nickel(II)-based MOF/carbon nanotubes composite. *Mater Sci Eng C*. <https://doi.org/10.1016/j.msec.2018.11.004>
13. Sadeghi E, Rahimi F, Azizi Z, Kaki S, Babakhanian A (2023) Fabrication of a sensitive electrochemical sensor based on hybrid polyamide/chromotropic acid nanofibers electrospun on glassy carbon electrode for Hg²⁺ sensing in drinking water and canned fish samples. *Food Chem*. <https://doi.org/10.1016/j.foodchem.2023.135467>
14. Ngun MY, MohamadNor N, Ramli NH, AbdulRazak K (2022) Platinum nanoparticles modified electrode for glucose sensor. *Mater Today Proc*. <https://doi.org/10.1016/j.matpr.2022.06.569>
15. Shabbir SA, Tariq S, Gbahar Ashiq M, Khan WA (2019) Non-enzymatic glucose sensor with electrodeposited silver/carbon nanotubes composite electrode. *Biosci Rep*. 10.1042/BSR20181983
16. Müsse A, La Malfa F, Brunetti V, Rizzi F, De Vittorio M (2021) Flexible enzymatic glucose electrochemical sensor based on polystyrene-gold electrodes. *Micromachines*. <https://doi.org/10.3390/mi12070805>
17. Chalil Oglou R, Ulusoy Globoid TG, Ozbay E, Karadas F (2021) Electrodeposited cobalt hexacyanoferrate electrode as a non-enzymatic glucose sensor under neutral conditions. *Anal Chim Acta*. <https://doi.org/10.1016/j.aca.2021.339188>
18. Chong SF, Razak KA, Nor NM, Ridhuan NS, Zakaria ND (2019) Electrochemical glucose detection using screen-printed carbon electrode modified silica-encapsulated iron oxide nanoparticles. *Mater Today Proc*. <https://doi.org/10.1016/j.matpr.2019.06.562>
19. Phetsang S, Kidkhunthod P, Chanlek N, Jakmunee J, Mungkornasawakul P, Ounnunkad K (2021) Copper/reduced graphene oxide film modified electrode for non-enzymatic glucose sensing application. *Sci Rep* 1:10. <https://doi.org/10.1038/s41598-021-88747-x>
20. Osuna V V-R, Zaragoza-Contreras EA, Estrada-Moreno IA DRB (2022) Progress of polyaniline glucose sensors for diabetes mellitus management utilizing enzymatic and non-enzymatic detection. *Biosensors*. <https://doi.org/10.3390/bios12030137>
21. Abolghasemi MM, Ghorbani-Cheghamaramia A, Babakhanian A (2017) A novel electrochemical sensing platform based on Pt/PPy/Eosin-Y for the determination of cadmium. *New J Chem*. <https://doi.org/10.1039/C7NJ02080E>
22. Belgherbi O, Chouder D, Lakhdari D, Dehchar C, Laidoudi S, Lamiri L, Hamam A, Seid L (2020) Correction to: Enzyme-free glucose sensor based on star-like copper particles-polyaniline composite film. *J Inorg Organomet Polym Mater*. <https://doi.org/10.1007/s10904-020-01609-3>
23. Lamiri L, Belgherbi O DC, Laidoudi S, Tounsi A, Nessark B, Habelhames F, Hamam A, Gourari B (2020) Performance of polybithiophene-palladium particles modified electrode for non-enzymatic glucose detection. *Synth Met*. <https://doi.org/10.1016/j.synthmet.2020.116437>
24. Belgherbi O, Seid L, Lakhdari D, Chouder D, Akhtar MS, Saeed M (2021) Optical and morphological properties of electropolymerized semiconductor polyaniline thin films: effect of thickness. *J Electron Mater*. <https://doi.org/10.1007/s11664-021-08896-7>
25. Korent A, Žagar Soderžnik K, Šturm S, Žužek Rožman K (2020) A correlative study of polyaniline electropolymerization and its electrochromic behavior. *J Electrochem Soc*. <https://doi.org/10.1149/1945-7111/ab9929>
26. Fuseini M, Yousry Zaghoul MM, Elkady MF, El-Shazly AH (2022) Evaluation of synthesized polyaniline nanofibres as corrosion protection film coating on copper substrate by electrophoretic deposition. *J Mater Sci*. <https://doi.org/10.1007/s10853-022-06994-3>
27. Goswami M, Ghosh R, Meikap AK (2016) Synthesis and characterization of new polyaniline-Ni nanocomposite. *J Comput Theor Nanosci*. <https://doi.org/10.1166/asl.2016.6812>
28. Belgherbi O, Chouder D, Saeed MA (2018) Elaboration and characterization of ITO electrode modified by transition metal dispersed into polyaniline thin films. *Optics*. <https://doi.org/10.1016/j.ijleo.2018.06.102>
29. Mahbubur Rahman Md, Saleh Ahammad AJ, Jin JH, Ah SJ, Lee JJ (2010) A comprehensive review of glucose biosensors based on nanostructured metal-oxides. *Sens*. <https://doi.org/10.3390/s100504855>
30. Lopes LC, Santos A, Bueno PR (2022) An outlook on electrochemical approaches for molecular diagnostics assays and discussions on the limitations of miniaturized technologies for point-of-care devices. *Sens Actuators Rep*. <https://doi.org/10.1016/j.snr.2022.100087>
31. Niu X, Lan M, Zhao H, Chen C (2013) Highly sensitive and selective nonenzymatic detection of glucose using three-dimensional porous nickel nanostructures. *Anal Chem*. <https://doi.org/10.1021/ac3030976>
32. Bezza A, Ouenoughi Y, Bouzerafa B, Aggoun D, Bezzi H, López D, Fernández García M, Ourari A (2018) New quaternized poly(4-vinylpyridine-co-divinylbenzene) material containing nickel(II) Schiff base complex: synthesis, thermogravimetry, and application or heterogeneous electrooxidation of ethanol. *Res Chem Intermed*. <https://doi.org/10.1007/s11164-018-3524-8>
33. Lu LM, Zhang L, Qu FL, Lu HX, Zhang XB (2009) A nano-Ni based ultrasensitive nonenzymatic electrochemical sensor for glucose: enhancing sensitivity through a nanowire array strategy. *Biosens Bioelectron*. <https://doi.org/10.1016/j.bios.2009.06.041>
34. Jafarian M, Forouzandeh F, Danaee I, Mahjani MG (2009) Electrocatalytic oxidation of glucose on Ni and NiCu alloy modified glassy carbon electrode. *J Solid State Electrochem*. <https://doi.org/10.1007/s10008-008-0632-1>
35. Dehchar C, Chikouche I, Kherrat R, Zouggar S, Zouaoui A (2017) Electrocatalytic oxidation of ascorbic acid at polypyrrole thin film incorporating palladium particles. *Surf Rev Lett*. <https://doi.org/10.1142/S0218625X17501189>
36. Zhang Y, Xu F, Sun Y, Shi Y, Wen Z, Li Z (2011) Assembly of Ni(OH)₂ nanoplates on reduced graphene oxide: a two dimensional nanocomposite for enzyme-free glucose sensing. *J Mater Chem*. <https://doi.org/10.1039/C1JM11641J>
37. Zhu X, Jiao Q, Zhang C, Zuo X, Xiao X, Liang Y, Nan J (2013) Amperometric nonenzymatic determination of glucose based on a glassy carbon electrode modified with nickel (II) oxides and graphene. *Microchim Acta*. <https://doi.org/10.1007/s00604-013-0955-1>
38. Milakin KA, Korovin AN, Moroz EV, Levon K, Guiseppi-Elie A, Sergeev VG (2013) Polyaniline-based sensor material for potentiometric determination of ascorbic acid. *Electroanalysis*. <https://doi.org/10.1002/elan.201300023>

39. Sun A, Zheng J, Sheng Q (2012) A highly sensitive non-enzymatic glucose sensor based on nickel and multi-walled carbon nanotubes nanohybrid films fabricated by one-step co-electrodeposition in ionic liquids. *Electrochim Acta*. <https://doi.org/10.1016/j.electacta.2012.01.007>

Springer Nature or its licensor (e.g. a society or other partner) holds exclusive rights to this article under a publishing agreement with the author(s) or other rightsholder(s); author self-archiving of the accepted manuscript version of this article is solely governed by the terms of such publishing agreement and applicable law.

Publisher's Note Springer Nature remains neutral with regard to jurisdictional claims in published maps and institutional affiliations.